

Proceedings of the Korean Nuclear Spring Meeting
Gyeongju, Korea, May 2003

Mobile Cargo Container Inspection System Using 450kVp X-ray

^aSung-Woo Kwak, ^aGyuseong Cho, ^bYun Yi, ^cInsu Kim, ^cBumsoo Han and ^dSung Min Goh

^aKAIST 373-1 Kusong-dong, Yusong-gu, Daejeon 305-701

^bGraduate School of Biotechnology, Korea University, Seoul 136-701

^cEB-Tech Co., Ltd. 103-6 Munji-dong, Yusong-gu, Daejeon 305-380

^dChonbuk National University, Chonju 561-756

Abstract

X-ray inspection system has been used for the inspection of illegal drugs, agricultural products and other contraband in custom application, and for the inspection of weapons and explosives in security application. This paper presents how to design and construct mobile cargo container inspection system using medium energy X-ray from the generic generator operated at 450 kVp. Particularly, X-ray detector design is treated relatively in detail, since there are few papers on X-ray detector design for rapid and nonintrusive container inspection system. From the image obtained with the inspection system developed in this paper, it turns out that the system can distinguish the object of 5mm in size and of 4% difference in density from the background. The design method of this study may be applied to X-ray inspection system using higher energy.

1. INTRODUCTION

The number of cargo containers used for export and import via land, sea and air have largely increased with world-wide economy. In such situation the cargo container inspection system is required to examine rapidly suspected objects without impeding the flow of container through ports in addition to the capability of detecting illicit substance and contrabands hidden in containers. In order to meet these operational constraints, X-ray technology has been studied and realized by several companies such as Heimann, AS&E, Perkin Elmer, Rapiscan and Tsinghua Tongfang, etc. [1], [2]. As a result, X-ray inspection system nowadays has being used for the detection of illegal drugs, agricultural products and other contrabands in custom application, and for the detection of weapons and explosives in security application.

Even though X-ray technology has played a significant role in various fields, there are few reports that involve the full treatment of the X-ray and light transport in detector design for medium and high energy X-ray detection. We have developed mobile cargo container

inspection system using 450 kVp X-ray. 450 kVp X-ray inspection system has been chosen under the consideration of the mobility between different ports of entry sites and the detectability of agricultural products smuggled into Korea from other countries. This work presents how to determine the parameters of X-ray detector components such as a scintillator, a photodiode with p-i-n structure (PIN photodiode) and a preamplifier of data acquisition system for 450 kVp X-ray detection. Behaviors of X-rays and lights in scintillator (CdWO₄, CWO) are taken into account in detector design. Based on our design, a prototype system has been constructed and technical feasibility and overall performance of the system was evaluated. The results will be feedback to more effective optimal designs for complete system.

2. DESIGN AND FABRICATION OF EACH COMPONENT

2.1 Determination of Geometry of CWO Element

Due to large X-ray absorption efficiency and low after-glow, CWO has been used in detecting high energy X-ray with fast scanning time even though it has low light output. Therefore, it is important to increase the light collection efficiency in the given geometry of CWO in order to achieve high signal-to-noise ratio (SNR). There are several factors to have an influence on the light output such as X-ray energy and irradiation direction, geometry and surface treatment of scintillator. In use for medical CT (Computed Tomography), a photodiode as a photosensor is bonded to the surface opposite to the side of scintillator where X-ray enters, while a photodiode-based detector for industrial application like nonintrusive container inspection system and industrial CT is placed parallel to the X-ray incident direction as shown in Fig.1 because X-ray used in industrial fields is highly energetic. In Fig.1, both X-ray absorption and light collection in scintillator for medical CT have the same exponential behavior according to the depth of the penetration of X-ray. The light collection efficiency is not the function of the penetration of X-ray. Thus, in order to calculate light output from CWO, both X-ray absorption and light collection efficiency should be considered.

Visible lights generated by X-ray absorption within the scintillator undergo scattering and absorption in bulk and reflection on surface. Then, lights are collected by photodiode optically coupled to the scintillator. Assuming generation of the monoenergetic light photon when the X-ray is absorbed, the total number of lights escaping from the scintillator can be simply given by

$$N = \int_E \int_V wEA(\vec{r}, E)h(\vec{r}, E)dv dE \quad (1)$$

In (1), N is the average number of photons produced per the absorbed energy keV, $A(\vec{r}, E)$ is the efficiency of energy deposition in the CWO, and $h(\vec{r}, E)$ describes the light collection efficiency, that is, the fraction of light transmitted through the scintillator-exit-window. V is volume of scintillator and E is X-ray energy.

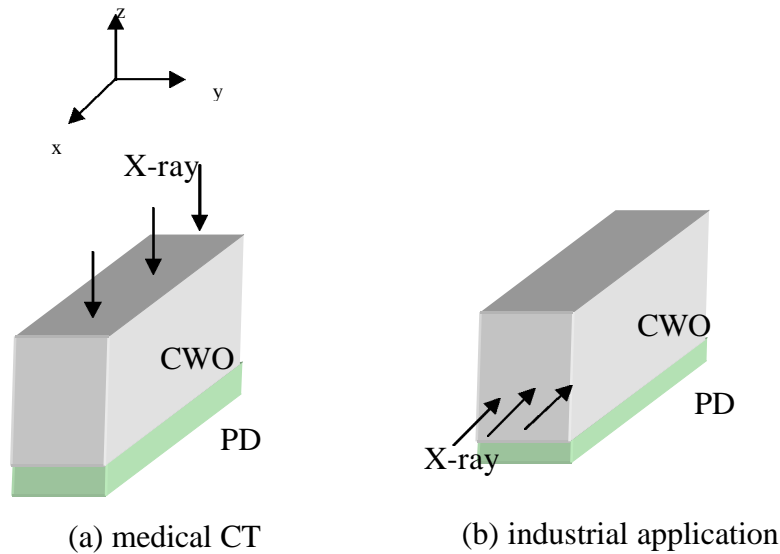


Fig. 1. Comparison of irradiation direction for medical CT and industrial application. The scintillator coupled to a photodiode is placed parallel to X-ray incident direction.

The final light output escaping from the CWO can be determined by the light generation process by interacting X-rays with the scintillator and the light escaping process from the CWO. These processes are treated separately to calculate the total number of lights escaping the CWO. Two Monte Carlo simulation codes are used; MCNP4B (Monte Carlo N-particle Transport Code) [3] for X-ray and DETECT97 for light transports, respectively [4]. In order to calculate the deposited energy as a function of geometry of the CWO, the overall CWO region is divided into small subregion with the size of 0.2 mm, which is smaller than mean free path of 150 keV photon [5]. The energy required to produce a light in CWO is about 67eV. That is, the mean number of lights produced per keV absorbed is about 15 (≈ 15 lights/keV) [6]. The number of lights generated in each subregion could be obtained by using the calculated energy deposition and the light yield. For simplicity it was assumed that the lights were generated at the center of each subregion. This assumption is reasonable because the difference between light collection efficiencies when the light is generated at the top or at the bottom of 1.7 mm x 3.0 mm x 10.0 mm CWO is estimated to be about 2% by computer simulation. According to (1), the total number of lights escaping from overall CWO block could be calculated by integrating the product of the generated photon number and collection efficiency over each subregion of the CWO. 450 kVp X-ray spectrum was calculated using MCNP4B under the consideration of X-ray generator structure, and it is shown in Fig.2 and normalized to the area of unity.

External reflector has been used to prevent the lights escaping from the crystals. Three types of surface treatment of CWO, that is, 4 ground sides/ground top, 4 polish sides/polish top and 4 polish sides/ground top, were simulated to investigate their effects on light output. Top-side surface means the surface of CWO opposite to the photodiode.

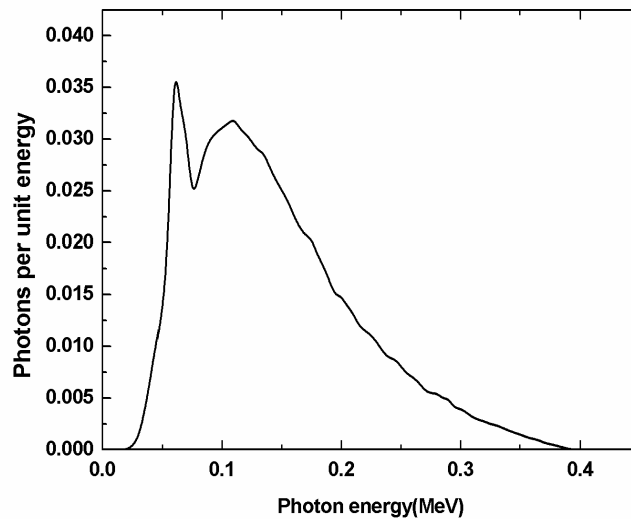


Fig. 2. Normalized spectrum of 450 kVp X-ray. 450kVp X-ray spectrum is calculated by MCNP4B.

Fig.3, 4 and 5 show the effects of CWO geometry as well as the effects of surface treatment on light output. Fig.3 shows the effects of crystal width on the light output while the height and depth are fixed at 3.0 mm and 10.0 mm, respectively. As shown in Fig.3, light output increases with the increase of crystal width. The number of light escaping from CWO increases slowly beyond 2.0 mm and saturates about at 4 mm. A trade-off between a spatial resolution and a light output of detector should be considered in determining the detector design. Taking into account the slope of increasing amount of light depending on the crystal width and the spatial resolution of our system, the optimal width turns out to be about 1.7 mm. Fig.4 shows the effects of crystal height on the light output while keeping the width and length fixed at 1.7 mm and 10.0 mm, respectively. A peak appears at 3.0mm in Fig.4. Light output decreases beyond 3.0 mm because the light collection efficiency is reduced by the internal light trapping and self-absorption as the crystal height increases [7]. Fig.5 shows the effects of crystal depth on the light output with fixed width and height at 1.7 mm and 3 mm, respectively. In Fig.5, light output increases with the increase of crystal depth and saturates at 10 mm.

Three figures, Fig.3, 4 and 5 show that CWO with ground surfaces gives more lights than other two cases, which is different from the results proposed by previous studies. Some studies suggested that polished surface be more efficient [8],[9], while others reported that ground surface yielded more light [10], [11]. Depending on studies, different results come from the fact that the effects of the surface treatment on the light output are also function of several other variables such as the properties of crystal materials, the geometry of the crystal and the generation location of light in crystal. Our results indicate that in polished crystal, considerable amount of the scintillation light is internally trapped and could not reach the photodiode. Ground surfaces break up internal reflections and preferentially direct light down

toward the photodiode. Therefore, ground surface yields more lights than polished surface. Simulation results of this study show that the CWO of 1.7 mm(width) x 3.0 mm(height) x 10.0 mm(depth) with the surface treatment of 4 ground sides and ground top is optimal for detecting 450 kVp X-ray.

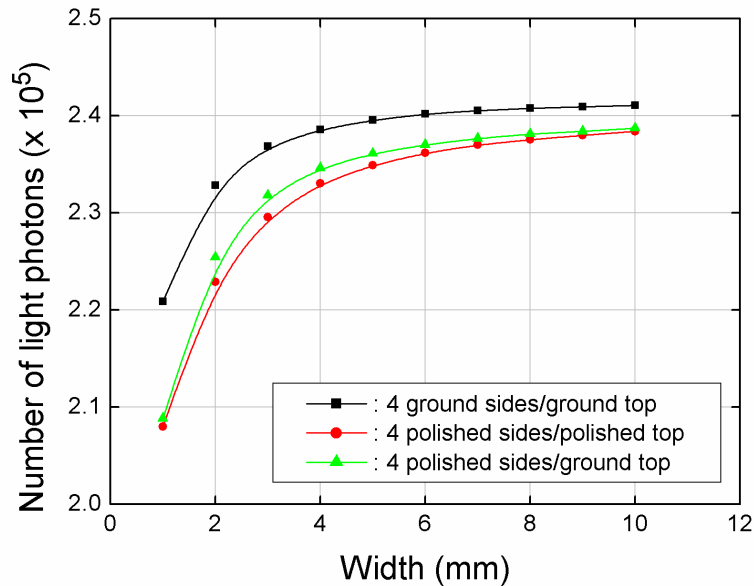


Fig. 3. Effects of crystal width on total light output in CWO. The increase of light output of CWO is slow beyond 2.0 mm. Ground surface yields more light than polished surface.

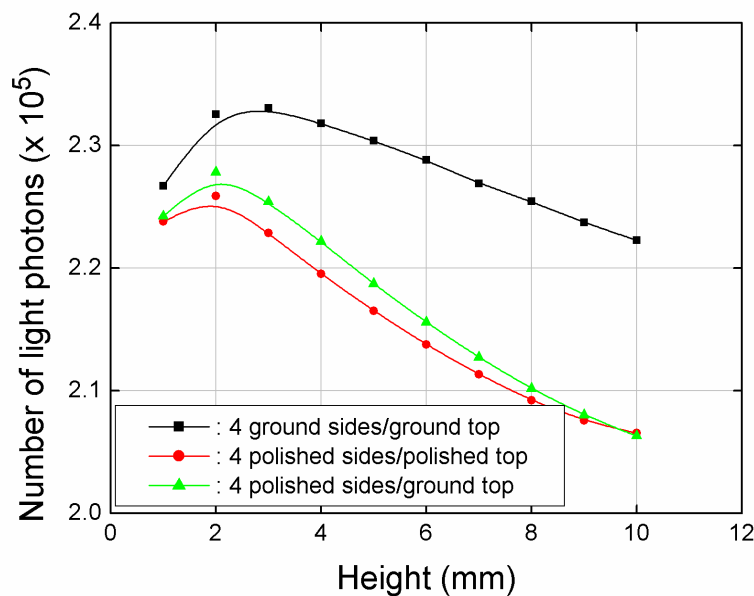


Fig. 4. Effects of crystal height on total light output in CWO. The light output of CWO shows maximum at about 3.0 mm. Ground surface yields more light than polished surface.

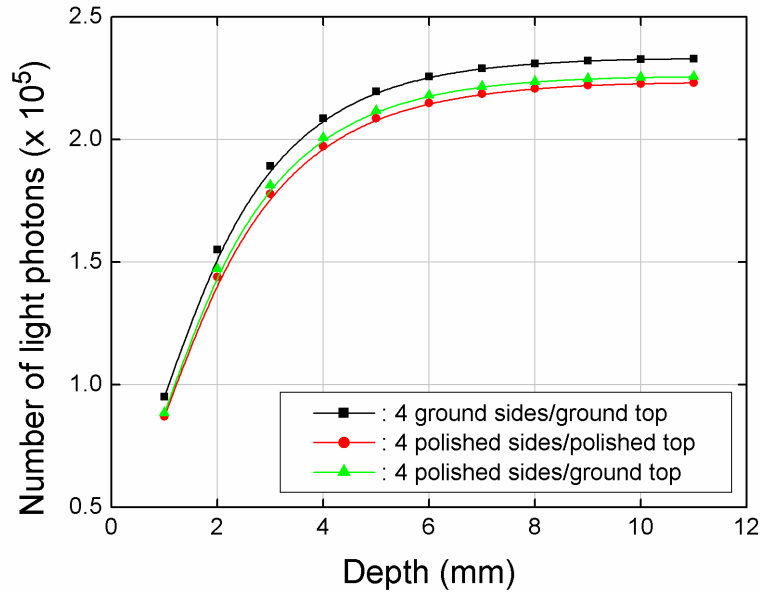


Fig. 5. Effects of crystal depth on total light output in CWO. The light output of CWO saturates at 10.0mm. Ground surface yields more light than polished surface.

2.2 Design and Fabrication of PIN Photodiode

PIN photodiode has been used as a photodetector detecting visible light emitted from scintillator. Due to the short wavelength of CWO light of 490 nm, the light is absorbed within a very shallow layer near surface before arriving at depletion layer and does not contribute to electric signal. Thus, in design of PIN diode for detection of light of CWO, it is important to make its p-layer as shallow as possible. In order to achieve a shallow junction, optimal conditions of ion implantation such as the thickness of SiO₂ oxide barrier, tilting angle of wafer with respect to incident ion beam and annealing conditions should be determined by computer simulations with the consideration of Si wafer properties like its orientation, resistivity and intrinsic impurity concentration.

(100) orientation has been chosen as PIN diode materials, since the penetration depth of boron ion in (100) is shallower than in (111) material [12]. Due to light weight of B⁺, the B⁺ has a long projected range(R_p) and a lower ionization rate. These lead to increase pn-junction depth. The BF₂(⁴⁹BF₂⁺) ion implantation was employed in this study because the R_p of BF₂ was about 25% of B and had higher ionization rate [13]. However, the BF₂ implantation induces some undesirable results like damages and deformations of crystalline lattice, then giving rise to an amorphous Si layer on the surface of Si crystal. This may cause recombination of carriers, and eventually adversely affect the diode performances like the increase of leakage current and the reduction of photosensitivity. This amorphous Si layer can be recrystallized and cured by subsequent annealing process. Also, there is a possibility of unwanted result that pn-junction depth deepens further during annealing. Optimal annealing conditions were estimated to be 750-900 °C and 30 minutes by computer simulations. If

annealing temperature is beyond 900 °C, boron doping profile has deepened dramatically. The PIN silicon photodiode was fabricated on 250 μm thick, n-type silicon substrates with high resistivity (1,200–4,000 Ω·cm). Fig.6 is the leakage current and capacitance of fabricated PIN photodiode measured as a function of the applied bias with a semiconductor parameter analyzer (HP 4155A). Fig.6 shows that a leakage current at 5 V and a capacitance without bias are about 1 nA/cm² and 550 pF/cm², respectively. In Fig.6, an abrupt increase in leakage current and capacitance is shown about 5 V. It is assumed that the abrupt increase may be due to an n⁺⁺-guard ring, which is heavily doped with a phosphorous impurity to reduce the leakage current of a photodiode. The depletion layers at two different interfaces of p⁺ layer-n⁻ intrinsic layer and n⁻ intrinsic layer-n⁺⁺ guard ring are deepened with reverse bias and at last are combined at 5 V together. The combination leads to the sharp increase of the two curves.

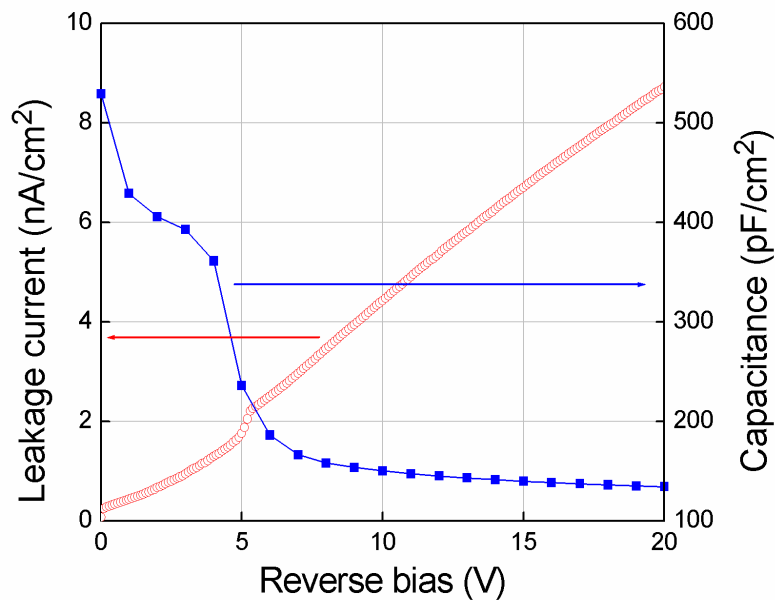


Fig. 6. Leakage current and capacitance of PIN diode developed in this study.

2.3 Data Acquisition System

Data Acquisition System (DAS), positioned between the detector array and the computer, performs the following three major functions; (1) amplifying the signal from detectors, (2) converting the analog signal into the digital, (3) transmitting the digital data to the computer for reconstruction and further image processing. DAS developed in this study could be physically divided into analog, digital and master board, image construction system. Analog board includes a dual switched integrator (ACF2101) as a preamplifier and a programmable gain instrumentation amplifier as buffered signal inverter [14]. A dual integrator (an odd integrator and an even integrator) was used in order to achieve the zero integration dead time for maximum utilization of detector signal during the continuous scan. While the detector signal charge was integrated in one integrator as shown in Fig.7, the signal in other integrator

was transmitted into the ADC through a MUX. Integration time of the integrator was designed to integrate the signal of 4 pulses of X-ray. Signal amplitude of our system was proportional to integration time and saturated almost at the period of 6 pulses duration. There is a trade-off between the signal amplitude of detector and the scan speed, in determining the integration time of the integrator in DAS. Signal information flow through DAS developed in this study is shown in Fig.8. The timing and control signal for integrators, the address signal of the MUX, the timing signal of ADC and the control signal of data transmission were generated in the digital logic board implemented by a FPGA which was coded with VHDL [15].

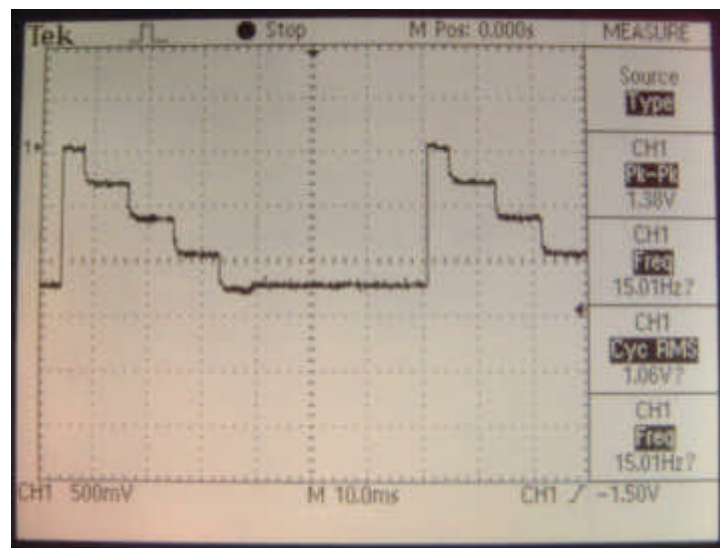


Fig. 7. 4 Pulse integration carried out by one of dual switched integrator. This figure shows that dual switched integrator integrates 4 pulses X-ray.

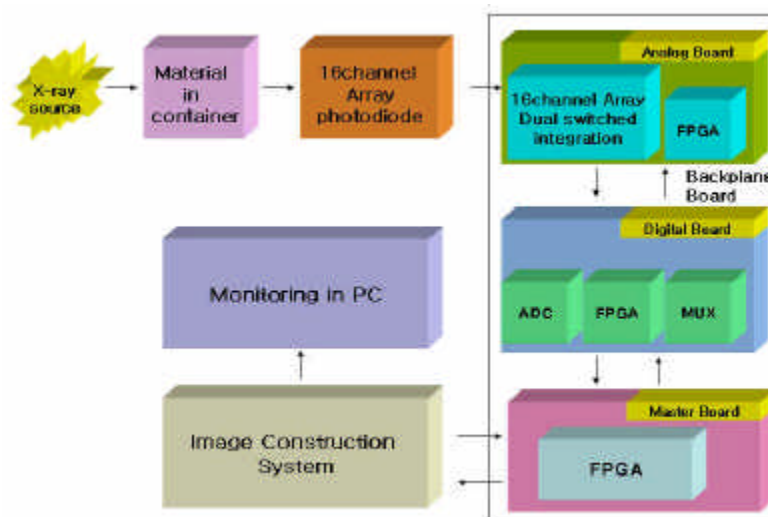


Fig. 8. Data acquisition system. DAS developed consists of analog, digital and master board, image construction system.

3. CONSTRUCTION OF MOBILE CARGO CONTAINER INSPECTION SYSTEM

Prototype mobile cargo inspection system has been constructed to evaluate the technical feasibility and performance of complex integrated system and finally to derive more effective optimal design parameters for complete system. X-ray inspection system consisted largely of a 450 kVp X-ray generator, a PIN photodiode-based linear detector array, a data acquisition system and an image construction system. Fig.9 shows prototype container inspection system developed. X-ray generator (CoRAD RG-450) produces pulsive 120Hz X-ray with maximum and average energies of 450 kVp and about 167keV, respectively. Tube current is about 10mA. A 16-channel detector array was made up of CWO scintillator elements, which were optically coupled to PIN photodiodes. Detector pitch was 2.0mm. To prevent crosstalk, TiO₂ spacer was inserted between the scintillators. 1.0 m(W) x 1.0 m(H)x 2.0 m(L) prototype container made of the same material with actual cargo container was prepared for inspection test as shown in Fig.9

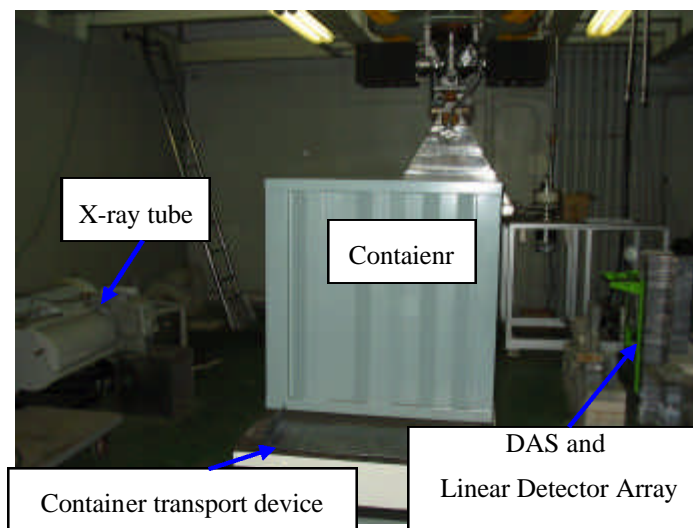


Fig. 9. Cargo container inspection system(Prototype). X-ray inspection system consisted of a 450 kVp X-ray generator, a PIN photodiode-based linear detector array, a data acquisition system and an image construction system.

4. CARGO CONTAINER INSPECTION TEST

Overall performance of the developmental system was evaluated. To test the spatial and contrast resolution, a variety of objects not only in shape but also in density were inserted in container. Objects include a plastic bottles filled partially with water, a liquor glass bottle, an iron plate with 2mm holes and different thicknesses, cement brick and so on. In this test, an

automatic transport device moved the container with constant speed of 8.0 cm/sec. Radiographic image of various objects obtained by the inspection system is shown in Fig.10. 5 mm holes is clearly seen. Image of empty part of plastic bottle has also been distinguished from the part filled with water. The contrast resolution can be said at least 4%, since the density of between air and plastic bottle detected is 4% different

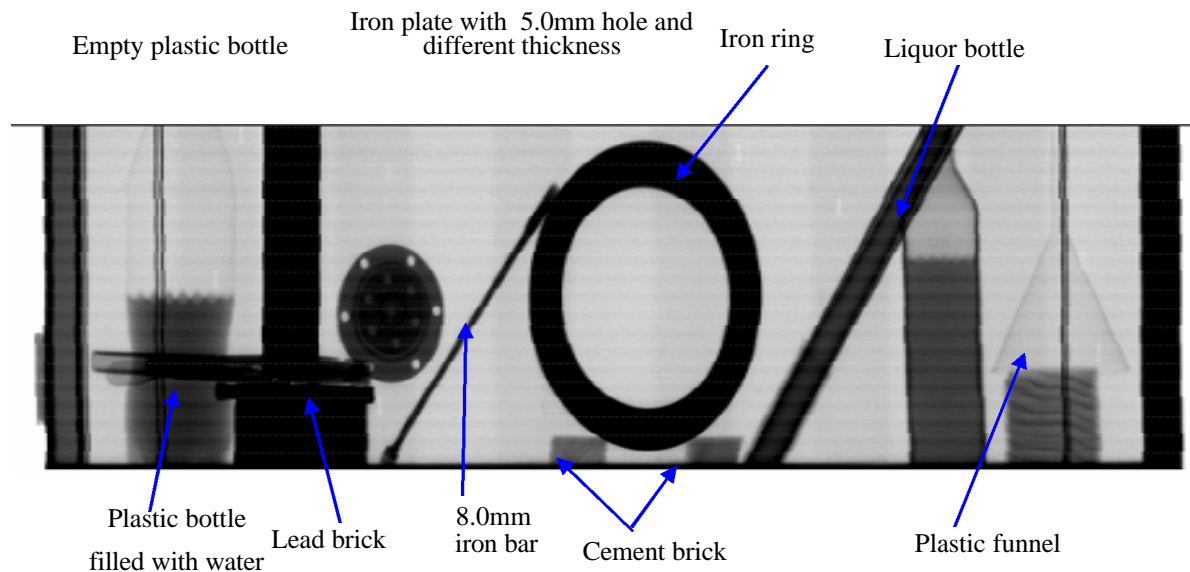


Fig. 10. Image of various objects in container. Inspection system developed has the spatial and contrast resolution of 5.0 mm and 4%, respectively

5. CONCLUSION

This paper has shown the method to design X-ray detector and total inspection system using 450 kVp X-ray. Design parameters determined in this study will be used in building total cargo container inspection system, and the methods of detector design can be applied to one for higher energy X-ray. In addition to scintillator array, PIN photodiode and DAS have also been optimized, and prototype cargo container inspection system using 450 kVp X-ray has been constructed in this study. Inspection system developed has the spatial and contrast resolution of 5.0 mm and 4%, respectively.

6. ACKNOWLEDGE

This work was supported by Ministry of Science and Technology of Korea Project No. M20206010001-02D0101-00310

7. REFERENCE

- [1] Hermann Ries, Fred Hemp and Cornelius Koch, "X-ray cargo inspection," *SPIE.*, vol. 2276, pp.234-241, 1994.
- [2] Roderick D. Swift and Roy P. Lindquist, "Medium energy X-ray examination of commercial trucks," *SPIE.*, vol. 2276, pp.242-254, 1994.
- [3] Judith F. Briesmeister (Ed.), *MCNP-A General Monte Carlo N-Particle Transport Code*, 1997.
- [4] G.F.Knoll and T.F.Knoll, *DETECT Manual*, University of Michigan, 1996.
- [5] W. Rossner and B.C. Grabmaier, "Phosphors for X-ray detectors in computed tomography," *J. Luminescence*, vol.48&49, pp29-36, 1991
- [6] Jeffrey Harold Siewerdsen, *Signal, Noise and Detective Quantum Efficiency of α -Si:H Flat-Panel Imagers*, University of Michigan, 1998, pp74-88.
- [7] C. Greskovich and S. Duclos, *Ceramic Scintillators*, GE Research and Development Center, Dec. 1996
- [8] Simon R. Cherry, Yiping Shao, Martin P. Tornai, Stefan Siegel, Anthony R. Ricci and Michael E. Phelps, "Collection of scintillation light from small BGO crystals," *IEEE Trans. Nucl. Sci.*, vol.42, no.4, pp1058-1063, Aug 1995.
- [9] Caesar E. Ordonez and Wei Chang, "Simulatin light output from narrow sodium iodine detectors," *IEEE Trans. Nucl. Sci.*, vol.44, no.3, pp1237-1241, Jun. 1997.
- [10] C.M. Ankenbrandt and E.M. Lent, "Increasing the light collection efficiency of scintillation counters," *Rev. Sci. Instr.*, vol.34, no.6, pp647-651, Jun. 1963
- [11] M.E. Globus and B.V. Grinyov, "Calculations of scintillators for radiation detector systems: dependence of spectrometric characteristics on shape, size, and reflector type," *IEEE Trans. Nucl. Sci.*, vol.142, no.4, pp357-360, Aug. 1995.
- [12] R. Hartmann, D. Hauff, P. Lechner, R. Richter, L. Struder, J. Kemmer and S. Krisch, "Low energy response of silicon pn-junction detector," *Nucl. Instr. and Meth. A*, vol.377, pp191-196, 1996.
- [13] Y. Saitoh, T. Akamine, K. Satoh, M. Inoue, J. Yamanaka and K. Aoki et al., "New profiled silicon pin photodiode for scintillation detector," *IEEE Trans. Nucl. Sci.*, vol.42, no.4, pp345-350, Aug. 1995.
- [14] *ACF2101 Application Bulletin*, Burr-Brown Co.
- [15] McCluskey, E. J., *Logic Design Principles with Emphasis on Testable Semicustom Circuits*, Prentice-Hall, Englewood Cliffs, N.J.,1986.